RAD Conference Proceedings, vol. 8, pp. 46–52, 2024
ISSN 2466-4626 (online) | DOI: 10.21175/RadProc.2024.10
www.rad-proceedings.org

RADIATION PROTECTION AT THE ELI BEAMLINES LASER FACILITY

Benoit Lefebvre*, Anna Cimmino, Dávid Horváth, Roman Truneček, Roberto Versaci, Srimanta Maity, Mihail Miceski, Alexander Molodozhentsev, Uddhab Chaulagain, Veronika Olšovcová

ELI Beamlines Facility, Extreme Light Infrastructure ERIC, Za Radnicí 835, 252 41 Dolní Břežany, Czech Republic

Abstract. *The ELI ERIC (Extreme Light Infrastructure European Research Infrastructure Consortium) aims at developing and operating the next generation of high-power laser systems in Europe. The Czech pillar of the consortium is the ELI Beamlines facility. It hosts world-class lasers with peak powers reaching 10 PW and repetition rates of up to 1 kHz. There, laser-driven beamlines deliver ultra-bright and ultra-short sources of X-rays, ions, and electrons for fundamental and applied research. Beam time is offered to users worldwide. The pulsed mixed radiation fields generated at the facility are challenging from a radiation protection standpoint. The facility beamlines feature cutoff energies reaching up to hundreds of MeV for ions and GeV for electrons. The beams are characterised by a broad spectrum with radiation delivered over an extremely short time structure, generally less than 1 ps. Furthermore, copious amounts of stray ionizing radiation are produced in reason of the intrinsic laser-matter interactions and beam scattering. An overview of radiation protection considerations at the facility is presented on the topics of radiation shielding and monitoring, and Monte Carlo simulation studies. Additionally, radiological case studies of beamlines under commissioning are presented.*

Keywords: *Laser-driven beamlines, Radiation protection, Monte Carlo simulation*

1. INTRODUCTION

The Extreme Light Infrastructure (ELI) is a European Research Infrastructure Consortium (ERIC) formally founded in 2021 which has for mission to enable scientists access to state-of-the-art lasers [1]. The consortium includes the Czech Republic and Hungary as host member countries, Lithuania and Italy as founding members, and Germany, Romania and Bulgaria as founding observers. The ELI ERIC manages laser facilities hosting some of the world's most powerful lasers, open to scientists worldwide for user experiments. The implementation of the facilities in host states started in 2011. The first user call was launched in 2022, shortly after the commissioning of the first experimental stations in the facilities. The Hungarian facility, ELI ALPS, is aimed at the study of ultrafast physics processes and attosecond measurement techniques. The Romanian facility, ELI NP, focuses on photonuclear physics and the study of exotic nuclei. Finally, the Czech facility, ELI Beamlines, the focus of these proceedings, hosts high-energy particle beams. The technologies which are developed at the facility could be applied for many applications ranging from medical imaging and radiotherapy to structure analysis in solid-state physics and molecular chemistry.

In these proceedings, we discuss radiation protection (RP) considerations at the ELI Beamlines facility and the challenges of dealing with ultra-fast and intense laser-driven sources. A general detailed review on the subject was already published in 2023 [2]. Here, we report on the latest developments put forward by the ELI Beamlines RP group. We start with a general description of the ELI Beamlines facility, presented in Section 2. A brief description of the facility's radiation sources is presented in Section 3. A summary of RP considerations at the facility is presented in Section 4. Finally, a selection of RP case studies illustrating the challenges addressed lately by the RP group is found in Section 5. These proceedings conclude in Section 6.

2. THE ELI BEAMLINES FACILITY

The ELI Beamlines facility has 4 flagship laser systems called, in order of increasing design peak power Allegra (10 TW) [3], Duha (100 TW) [4], HAPLS (1 PW) [5] and Aton (10 PW) [6]. The fastest repetition rate is achieved with Allegra at 1 kHz and the largest pulse energy is achieved by Aton at 1.5 kJ. All are custom laser systems developed with varying involvement from external institutes. These lasers produce very short light pulses, less than 150 fs with the fastest laser system, Allegra, featuring a pulse duration of just 15 fs.

All the ELI Beamlines flagship lasers drive experimental stations where ionizing pulsed radiation fields are generated. We list here some of these stations to provide an overview of the reach of the ELI Beamlines physics program. Only the stations producing the most intense radiation fields are described. The P3 plasma physics infrastructure aims at the study of fundamental physics under extreme conditions [7]. There, mixed high-energy radiation fields are generated at large emission angles. The ELIMAIA [8] beamline generates proton

*E-mail of the corresponding author: benoit.lefebvre@eli-beams.eu

or ion beams at planned energies exceeding 100 MeV/u. There, beams are generated by focusing the laser mainly on solid targets. The beams are transported by the ELIMED [9] section for energy selection, beam focusing and diagnostics, and handling of irradiated samples. The LUIS beamline aims at delivering incoherent photon beams (<10 keV) by undulating electron bursts generated by the Laser Wakefield Acceleration (LWFA) mechanism [10]. The ELBA beamline produces multi-GeV LWFA electron beams for fundamental science studies [11]. The Gammatron beamline delivers ultra-bright X-ray beams (<100 keV) generated by wiggling LWFA electrons in the target plasma Wakefield [12]. The station can also be configured to produce Inverse Compton scattering photons at energies of hundreds of MeV. Finally, the ALFA station delivers a high-rate (1 kHz) high-energy (cutoff energy of 50 MeV) and highly focused (<2 mrad) LWFA electron beam [13]. Beams with cutoff energies above 150 MeV are planned in a later development stage. Most experimental stations have been successfully commissioned and are ready to host user experiments [13]. Most stations outlined a multi-stage planning whereby beam parameters are improved during a series of technical upgrades. Almost all stations are located in one of the 5 experimental halls of the facility. The halls feature thick concrete (> 1 m) walls offering nominal shielding against radiation for the adjacent halls and control rooms.

3. Radiation sources

Pulsed and steady ionizing radiation sources are found in experimental areas of the facility. All pulsed sources are laser-driven with a time structure comparable to the laser pulse duration (<1 ps). The pulsed radiation fields include prompt radiation, originating directly from the laser target, and stray radiation, produced from a beam interaction with the beamline infrastructure or irradiated sample. Prompt radiation sources include protons and ions, with energies larger than 100 MeV/u and yield up to 10^{13} particles per burst at a repetition rate of up to 10 Hz. The facility LWFA beamlines can generate prompt multi-GeV electron bursts with yields reaching 200 pC. For all beamlines, intense stray radiation fields are expected. For example, Bremsstrahlung X-rays with cutoff energies reaching 10 MeV are produced by electron refluxing in solid laser targets at ELIMAIA. Stray radiation can also be produced by scattering of the primary beam in the beam transport system, collimators and magnets. Finally, beam termination by a detector, sample or beam dump generates stray radiation. Neutrons, electrons and photons are the most common particles generated from such interactions.

Steady radiation sources produce ionizing radiation over a much longer time scale. Such sources include, among others, activated material in the experimental halls. Long-term storage is allocated for such material in case their activity reaches an unacceptable level for the health of personnel working in the vicinity. Sealed sources are also routinely used by the RP group and experimental teams.

4. Radiation protection

The ELI Beamlines RP group is responsible for the radiological safety of the facility's personnel, the general public and the environment. It operates under the framework of the Czech legislation, which comprises the Atomic Act 263/2026 on the Peaceful Use of Nuclear Energy and Ionizing Radiation and 20 additional decrees [15]. The law is itself harmonized with directives of the European Atomic Energy Community (EURATOM) [16]. One of the most relevant requirements in the context of RP at ELI Beamlines concerns the exposure of radiation workers, which shall remain below the legal effective dose, that is, 20 mSv per year. In practice, the RP group established, in the spirit of "as low as reasonably achievable" (ALARA) principles, a more stringent limit of 1 mSv per year. In addition, more stringent limits were established at ELI Beamlines for exposure to the eye lens, skin and extremities. Among the main responsibilities of the RP group are the definition of controlled and supervised areas at the facility, in which the ambient radiation levels are monitored, and the management of contamination and activated material created as a result of experiments.

The RP group collaborates closely with experimental teams on experimental planning. In a typical case, the group is provided with a "source term", which consists of a detailed description of the radiation source including its spectrum, intensity, location and divergence. Operational parameters are also provided including the planned laser repetition rate and operation schedule. The source term drives the design of appropriate shielding or beam dumps at experimental stations, as well as to drive the establishment of appropriate protocols namely regarding worker's occupancy. This work is supported by Monte Carlo (MC) radiation transport simulations, which, based on the source term, provide estimates of the ambient dose equivalent, particle fluences, material activation and damage to electronics. The group uses preferably the FLUKA [17,18] software. The facility is a member of the FLUKA.CERN collaboration managing the support and development of the code.

High-power laser facilities are still novel radiation installations which brings many challenges for RP operations. The source term itself is often a source of scientific studies for experimental teams. It seldom provides a precise estimate of the radiation source characteristics during experiments, let alone at the planning stage. Therefore, continuous close collaboration with experimental teams is necessary in pair with radiation monitoring of the experiments. The latter is achieved with active radiation monitors in the corridors, control rooms and in the vicinity of selected shielding parts. In addition, optically stimulated luminescent dosimeters are deployed in the halls to measure the integrated dose at key

locations. Finally, users and staff alike are required to wear a personal electronic dosimeter during shooting when the production of ionizing radiation is possible.

5. Selected case studies

The RP group continuously provides expertise in radiation physics for the commissioning and running of experimental stations at the facility. The work accomplished lately is sizable. Therefore, for conciseness, we only present here a selection of the latest achievements of the group in two representative case studies.

5.1. LUIS Beamline RP assessment

The LUIS beamline aims at delivering incoherent undulator photon beams generated by the Self-Amplifier Spontaneous Emission (SASE) mechanism whereby the photon beam is created by the injection of an electron beam in an undulator. At LUIS, this is achieved using an LWFA electron beam with a peak energy of nominally 800 MeV transported into a multi-stage beamline and then injected into an undulator. The maximum energy of photons in the resulting SASE beam is lower than 10 keV, of little radiological concern. This case study will, therefore, concentrate exclusively on the electron beam. The goal of this radiological assessment is to evaluate the effectiveness of the shielding used and to estimate the activation rate of beamline components and shielding elements.

The first stage of the beamline is the interaction chamber, which hosts the gaseous laser target from which the electron beam originates. Beam focusing is carried out in the next stage which hosts 3 quadrupole magnets. Their field gradients are tuned such that the beam envelope is the narrowest at the centre of the undulator. The station also hosts two dipole magnets used to steer the beam. The next stage is the outcoupling chamber, where an optical system safely deflects the laser beam from the electron beam axis. A turbo-integrated current transformer (ICT) sensor, used to measure the beam charge, is installed just after the decoupling chamber. A collimator stage follows to shield the downstream undulator against the beam halo, mostly consisting of background electrons with a high divergence or outside of the main primary energy peak. It consists of a vertical steel slot of width 2 cm, height 6.2 cm and length 10.5 cm. The station also hosts a first (upstream) Beam Position Monitor (BPM) with its associated reference cavity used to measure the beam profile position. The next stage comprises the undulator, where electrons are wiggled by a series of permanent magnets to generate the desired SASE photons. The following stage hosts diagnostics for beam characterization including, among others, a downstream BPM. The next station is the electron spectrometer, where the electron beam is bent downwards by a permanent dipole magnet, hits a scintillation screen and is ultimately absorbed in a granite dump. The purpose of the spectrometer is twofold. Firstly, it provides a measurement of the electron beam spectrum and divergence deduced from the dispersion trace left on the scintillation screen. Secondly, it filters out electrons from the photon beam. Some off-peak electrons may, however, propagate past the spectrometer stage. Therefore, an X-ray mirror chamber is installed in the following station to bend the photon beam off-axis by 5 degrees. The photon beam terminates at an X-ray spectrometer station where it is characterized or used for sample irradiation. All stages of the LUIS beamlines have a combined length of 15 m. A 3D visualization of the LUIS beamline as rendered by the Flair software [19] is shown in Fig. 1. A granite far shielding, not shown in the visualization, is installed downstream to block a floor penetration leading to the control room against electrons propagating past the electron spectrometer.

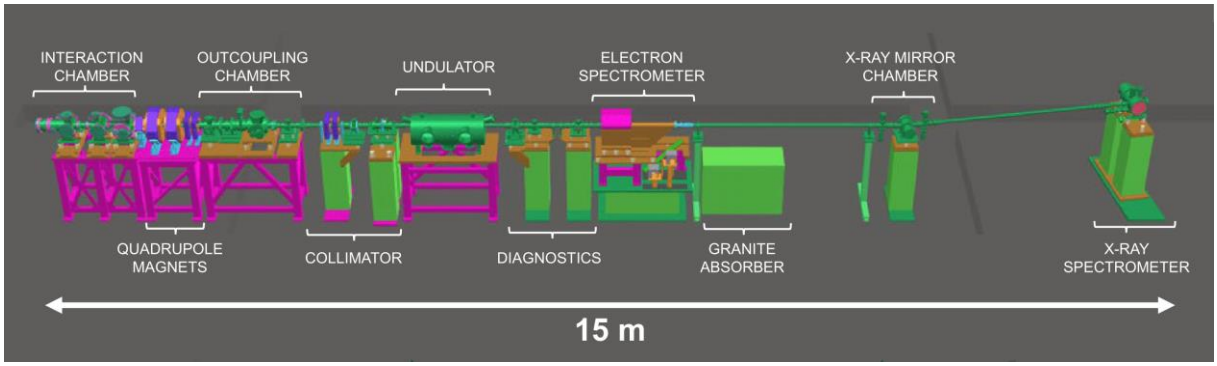

Figure 1. Simulation model of the LUIS beamline.

The source term used for MC simulation consists of Particle-in-Cell (PIC) simulation outputs carried out in 2D with the EPOCH software [20]. They contain the phase-space information (position and momentum) of electrons sampled just as they exit the laser target. The 2D phase-space was translated to 3D by uniformly sampling the azimuthal component of the electron position and momentum when generating primaries in the FLUKA simulation. It is useful to assess different operational scenarios to better anticipate the radiological impact of different possible experimental configurations. Therefore, two LWFA mechanisms were investigated: the self-injection (SI) and the ionization-injection (II)

regimes. A PIC output was used corresponding to each of these regimes. The physics underlying each scheme and their practical implementation fall outside the scope of these proceedings. For our purposes, it suffices to say that the self-injection regime is characterized by distinct energy peaks at 300 and 430 MeV (5 MeV RMS) while the ionization-injection energy spectrum is broadband between 50 and 650 MeV. For RP purposes the ionization-injection regime can be considered as a "worst-case" scenario because electrons outside of the energy peak for which the beamline was tuned will not be properly transported, namely at the quadrupole stage, and will scatter along the beamline rather than cleanly terminate in the electron spectrometer beam dump. The beam divergence is also highly relevant as off-axis electrons may not be properly focused as they are more likely to hit the beam pipe walls or other elements of the beamline. Electrons making up the 430 MeV peak in the SI regime can be divided into a "core" population, having a divergence of 2.8 mrad (73% of electrons) and a "background" component having a divergence of 12.7 mrad. To illustrate the effect of the different populations and LWFA mechanism, 4 simulation case studies were conducted:

a) SI regime with core component only.
b) SI regime with core and background components.
c) SI regime with full spectrum (both 300 and 430 MeV peaks).
d) II regime with full spectrum.

For the MC simulations of cases a) and b), the primary momentum direction and energy were sampled from normal distributions. For cases c) and d), the momentum and energy were attributed by randomly selecting electrons from the PIC output phase-space. Beam focusing was modelled by generating quadrupole fields in the effective volumes of the quadrupole magnets. The field gradient was tuned for an energy of 430 MeV, corresponding to the second peak of the SI regime spectrum. The fluence map of all particles for all case studies is shown in Fig. 2. A one-dimensional visualization of the fluence is shown in Fig. 3, just passed the upstream BPM, where the scored fluences are the highest. The results are normalized for a shot charge of 100 pC (6×108 electrons), an estimate of the beamline yield based on the results of the mentioned PIC simulations.

Activation studies were also conducted with FLUKA assuming a hypothetical campaign of 4 months with continuous shooting during 6-hour working days. Maps of H* are shown in Fig. 4 for cooldowns of 10 minutes and one year. Because the values of H* are very close to, and sometimes above 1 µSv/h, we conclude that great care should be taken for post-irradiation interventions carried out in the vicinity of the focusing stage, the Turbo-ICT, the BPM systems and the electron spectrometer. Furthermore, the ambient dose equivalent is very high inside the vacuum enclosure after the 10-minute cooldown. These results justify thorough post-irradiation surveys before permitting work in the hall. A one-year cooldown, however, appears sufficient to permit work anywhere in the hall, including in the beam pipe, with usual precautions.

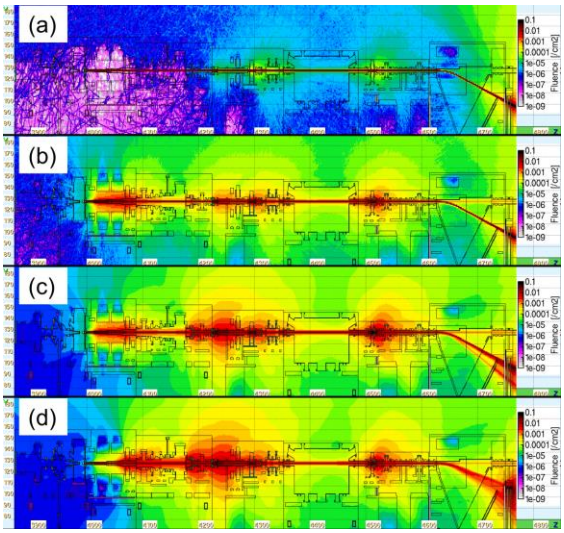

Figure 2. Simulated fluence of all particles along the beamline in the vertical plane for the case studies a)-d). The averaging range of the projection is ±10 cm from the beam axis.

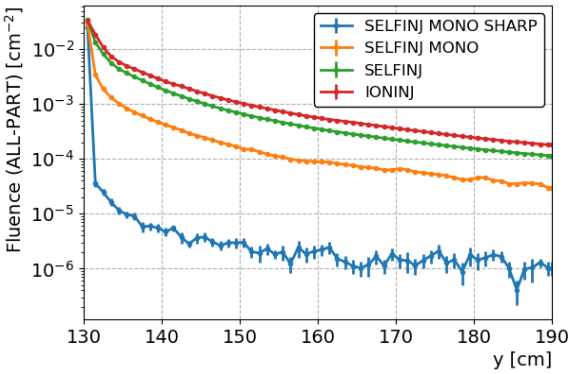

Figure 3. Fluence of all particles as a function of the vertical distance from the floor at the location of the upstream BPM. The beam axis is located at y=130 cm for simulation case studies a) SELFINJ MONO SHARP, b) SELFINJ MONO, c) SELFINJ and d) IONINJ.

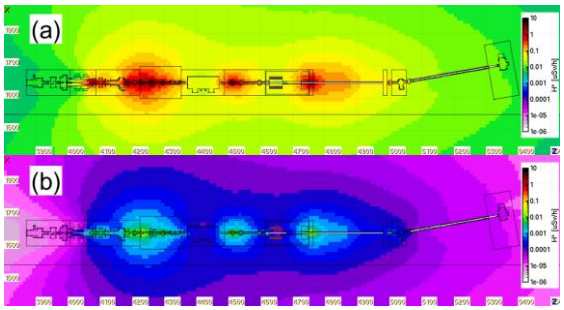

Figure 4. Post-irradiation ambient dose equivalent H* shown in the horizontal plane for a cooldown of (a) 10 minutes and (b) one year. The averaging range of the projection is ±25 cm from the horizontal beam plane.

5.2. Gammatron Beamline RP Assessment

At the Gammatron beamline, the laser is focused on a gas target to generate LWFA electron bursts. The beamline goal is to ultimately provide a photon beam with energies ranging from the keV level, generated in-situ by electron wiggling in the laser Wakefield, or up to a few hundreds of MeV, via the inverse Compton scattering mechanism [3].

While the photon beam propagates downstream of the interaction chamber in a dedicated beam pipe for sample irradiation, electron bursts are not needed for experiments. Therefore, they are filtered from the photons by a bending dipole magnet in the interaction chamber placed just after the gas target. The filtered electrons then propagate off-axis in the horizontal plane. Given their low energy, photons are completely stopped by the walls of the experimental halls. Therefore, they are of minor radiological concern and will not be further discussed. The electrons, however, require dedicated shielding to keep the radiation level outside the hall to an acceptable level.

For the shielding design, the electron spectrum is assumed to have a triangular shape going as $1-E_e/E_{pk}$ where E_e is the electron energy and E_{pk} is the cutoff energy. For this work, a conservative cutoff energy of 1.6 GeV is assumed, about twice the design energy. Furthermore, the electron burst divergence is assumed to be 5 mrad with a total charge of 200 pC (~10^9 electrons per laser shot). The origin of the electron beam is taken as the gas target, itself located 175 cm from the downstream wall of the interaction chamber. The bending magnet, of average strength 950 mT, is placed just a few cm from the target.

It is useful to separate the electron spectrum into three distinct parts. Electrons with energies lower than 20 MeV are fully stopped by the 4 cm thick interaction chamber walls made of an aluminum alloy (EN5083). Electrons with moderate energies, in the range of 20 to 100 MeV, are strongly bent by the magnetic field and propagate towards the side and corner of the interaction chamber. There, it was chosen to install a lead shield of thickness varying between 1 and 2 cm. The lead plates are covered with stainless steel cladding to protect against metal toxicity. The 1 cm thick plates are installed in an extruded aluminum structure standing on an adjacent optical breadboard table used for diagnostics. The 2 cm thick plates are installed on a rolling frame also made of extruded aluminum. The frame can be drawn to the side to facilitate access to instruments. Moreover, it is equipped with an interlock key connected to the laser interlock system, which ensures its proper positioning before beamline operation is enabled. Finally, electrons with energies in the range of 100 MeV to 1.6 GeV miss by just a few cm the photon beam pipe. To fully absorb these electrons, a much thicker shield is needed. For this purpose, a beam dump was designed made of a 25 cm thick and 100 cm wide steel core inserted in a granite structure. The core height is 10 cm to fully cover the electron beam transverse profile. Polyethylene sheets of thickness varying between 5 and 10 cm are installed around the granite structure and steel core to shield against neutrons produced inside the dump. The photon beam pipe is surrounded by a steel sleeve inserted in the granite structure to shield against scattering in this region. The dump extends from the side lead shield to the photon beam pipe for a total width of 145 cm. A clearance of 30 cm is left between the dump and the interaction chamber.

Simulation studies of the shielding were carried out using FLUKA. The magnetic field inside the bending magnet was modelled using field survey data. The 3D simulation model of the dump as rendered by Flair is shown in Fig. 5. To illustrate the effect of the bending magnet and the effectiveness of the shielding, a horizontal electron fluence map is shown in Fig. 6. As for the previous case study, the value of the ambient dose equivalent H* was scored in the surrounding corridors and the control room. An average of 180 laser shots per hour is assumed for normalization. The scored H* values are several orders of magnitude below 1 μSv/h except in areas close to hall penetrations where they approach 1 μSv/h. These penetrations are large openings in the hall walls necessary for laser beam transport pipes. The concerning penetrations consist of 3 m x 3 m openings located 3.5 m up from the hall floor which communicate with the adjacent halls. Radiological hazards should therefore be considered when carrying out work at heights in the adjacent halls during Gammatron shooting.

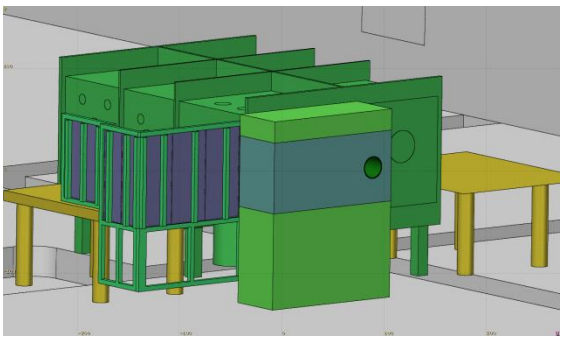

Figure 5. 3D model of the Gammatron beamline shielding simulation model as rendered by Flair with the photon beam pipe removed for better visibility.

Given the high energy of electrons stopped by the dump, activation of the steel dump core is expected. For that reason, the core was segmented into smaller steel slabs of cross-section 5 cm × 10 cm. The slabs can be fitted with hooks for easier and safer handling. The activation of the dump was also estimated with FLUKA assuming 10 hours of daily shooting during a campaign of 4 months. According to the simulation, the first upstream slab of the core would be considered radioactive waste by the Czech legislation even after a one-year cooldown

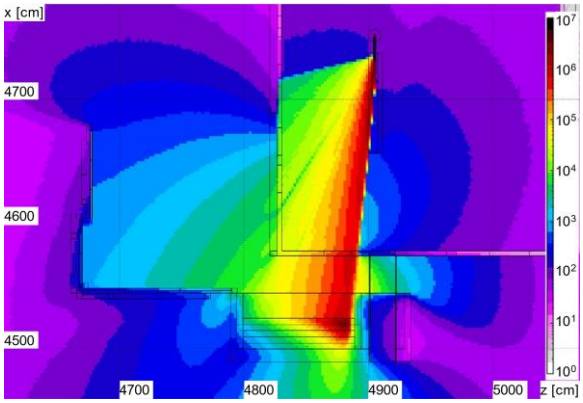

Figure 6. Fluence of electrons in cm-2 per laser shot. The averaging range of the projection is ±25 cm from the horizontal beam plane.

The post-irradiation ambient dose equivalent was also calculated after a 10-minute cooldown and is shown in Fig. 7. Work carried out outside of the dump should be safe, but a longer cooldown is prescribed when the dismantling of the dump is necessary. An annual or biannual replacement of the core slabs could be required depending on the true shooting schedule. An activation monitor is currently installed on the dump to follow the onset of activation in real time.

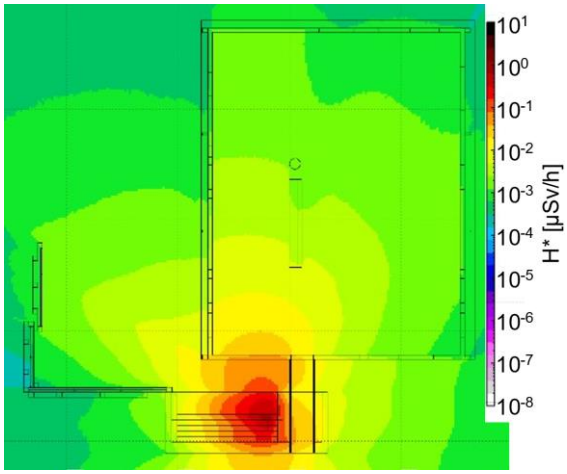

Figure 7. Ambient dose equivalent H* in µSv/h after a 10-minute cooldown following a 4-month campaign.

6. Conclusion

The RP group of the ELI Beamlines facility strives to ensure the radiological safety of the scientific staff and visiting users with state-of-the-art procedures and equipment. The group routinely advises scientific teams on the topic of radiation physics, instrumentation and MC simulation. The case studies presented in these proceedings can attest to this continuous collaboration. The simulations also help the group to better plan interventions, in particular in a facility with very unusual radiation sources. The LUIS and Gammatron beamlines are both in an advanced stage of commissioning, the latter already accepting proposals for user experiments. Work is in progress to evaluate the true effectiveness of the radiation shielding installed based on readings of the monitoring system and temporary ambient dosimeters.

The case studies revealed that radiological conditions at the facility depend heavily on the true quality of the delivered beam, which can be unpredictable even at state-of-the-art laser-driven beamlines. Additionally, operational factors such as quadrupole field gradients and the placement of bending magnets may influence yields of stray radiation. Effective radiological planning at laser facilities requires careful consideration of the source term and a thorough understanding of the beamline infrastructure. RP practitioners should collaborate closely with experimentalists throughout beamline development, commissioning and routine operation to refine radiological assessments and update safety protocols as needed.

References

1. G. Korn et al., “ELI - Extreme Light Infrastructure Whitebook”, Science and Technology with Ultra-Intense Lasers, THOSS Media GmbH, 2011. https://eli-laser.eu/media/1019/eli-whitebook.pdf
2. A. Cimmino et al., “Radiation Protection at Petawatt Laser-Driven Accelerator Facilities: The ELI Beamlines Case”, *Nucl. Scienc. Eng.*, vol. 198, no. 2, 245–263, 2024. https://doi.org/10.1080/00295639.2023.2191585
3. F. Batysta et al., “Pulse synchronization system for picosecond pulse-pumped OPCPA with femtosecond-level relative timing jitter”, *Opt. Express*, vol. 22, no. 2, pp. 106-30281-30286, 2014. https://doi.org/10.1364/OE.22.030281
4. J. T. Green et al., “L2-DUHA 100 TW High Repetition Rate Laser System at ELI-Beamlines: Key Design Considerations”, *Rev. Laser Eng.*, vol. 49, no. 2, pp. 106-109, 2021. https://doi.org/10.2184/lsj.49.2_106
5. E. Sistrunk et al., “All Diode-Pumped, High-repetition-rate Advanced Petawatt Laser System (HAPLS)”, *Conference on Lasers and Electro-Optics*, *OSA Technical Digest*, 2017, paper STh1L.2. https://doi.org/10.1364/CLEO_SI.2017.STh1L.2
6. F. Batysta et al., “Spectral pulse shaping of a 5 Hz, multi-joule, broadband optical parametric chirped pulse amplification frontend for a 10 PW laser system”, *Opt. Lett.*, vol. 43, no. 16, pp. 3866-3869, 2018. https://doi.org/10.1364/OL.43.003866
7. S. Weber et al., “P3: an installation for high-energy density plasma physics and ultra-high intensity laser-matter interaction at ELI-Beamlines”, *Matter Radiat. Extremes*, vol. 2, pp. 149-176, 2017. https://doi.org/10.1016/j.mre.2017.03.003
8. F. Schillaci et al., “The ELIMAIA Laser–Plasma Ion Accelerator: Technological Commissioning and Perspectives”, *Quantum Beam Sci.*, vol. 6, no. 4, pp. 30-1-23, 2022. https://doi.org/10.3390/qubs6040030
9. G.A.P. Cirrone et al., “ELIMED-ELIMAIA: The First Open User Irradiation Beamline for Laser-Plasma-Accelerated Ion Beams”, *Front. Phys.*, vol. 8, pp. 564907-1-8, 2020. https://doi.org/10.3389/fphy.2020.564907

10. E. A. Vishnyakov et al., "Compact undulator-based soft x-ray radiation source at ELI Beamlines: user-oriented program", *Proc. SPIE 12582, Compact Radiation Sources from EUV to Gamma-rays: Development and Applications*, 12582, pp. 1258209-1-10, 2023. https://doi.org/10.1117/12.2665377
11. G. Grittani et al., "ELI-ELBA: fundamental science investigations with high power lasers at ELI-Beamlines", *OSA High-brightness Sources and Light-driven Interactions Congress, Optica Publishing Group*, JM3A.20, 2020. https://doi.org/10.1364/EUVXRAY.2020.JM3A.20
12. U. Chaulagain et al., "ELI Gammatron Beamline: A Dawn of Ultrafast Hard X-ray Science", *Photonics*, vol. 9, no. 11, pp. 853-1-23, 2022. https://doi.org/10.3390/photonics9110853
13. C.M. Lazzarini et al., "Ultrarelativistic electron beams accelerated by terawatt scalable kHz laser", *Phys. Plasmas*, vol. 31, no. 3, pp. 030703-1-6, 2024. https://doi.org/10.1063/5.0189051
14. Extreme Light Infrastructure ERIC, "ELI User Portal", Website (current as of Oct. 31, 2024) URL: https://up.eli-laser.eu
15. Státní úřad pro jadernou bezpečnost, "Atomic Law", (current as of Oct. 31, 2024) (in Czech). https://www.sujb.cz/legislativa/atomove-pravo
16. Member States of the European Union, "Consolidated version of the Treaty establishing the European Atomic Energy Community", OJ C 203, 7.6.2016, p. 1–112, 2016. http://data.europa.eu/eli/treaty/euratom_2016/oj
17. C. Ahdida et al, "New Capabilities of the FLUKA Multi-Purpose Code", *Front. Phys.*, vol. 9, pp. 788253-1-14, 2022. https://doi.org/10.3389/fphy.2021.788253
18. G. Battistoni et al., "Overview of the FLUKA code", *Ann. Nucl. Energy*, vol. 82, pp. 10-18, 2015. https://doi.org/10.1016/j.anucene.2014.11.007
19. V. Vlachoudis, "FLAIR: A Powerful But User Friendly Graphical Interface For FLUKA", in *Proc. Int. Conf. on Mathematics, Computational Methods & Reactor Physics*, 2009. https://cds.cern.ch/record/2749540
20. T.D. Arber et al., "Contemporary particle-in-cell approach to laser-plasma modeling", *Plasma Phys. Control. Fusion*, vol. 57, no. 11, pp. 113001-1-26, 2015. https://doi.org/10.1088/0741-3335/57/11/113001
21. C. Sneha, "ICRU report 95 - Operational quantities for external radiation exposure", *Rad. Prot. Env.*, vol. 44, no. 2, pp. 116-119, 2021. https://dx.doi.org/10.4103/rpe.rpe_38_21